Flv1-4 proteins function in versatile combinations in O_2 photoreduction in cyanobacteria

Anita Santana-Sánchez, Daniel Solymosi, Henna Mustila[1], Luca Bersanini[2], Eva-Mari Aro*, Yagut Allahverdiyeva*

Molecular Plant Biology, Department of Biochemistry, University of Turku, FI-20014, Finland

[1]Present address: Department of Chemistry-Ångström Laboratory, Uppsala University, SE 75120 Uppsala, Sweden

[2] Present address: Biophysics of Photosynthesis, Department of Physics and Astronomy, Vrije Universiteit Amsterdam, 1081 HV Amsterdam, The Netherlands

* For correspondence: allahve@utu.fi (YA); evaaro@utu.fi (EMA)

Abstract

Flavodiiron proteins (FDPs) constitute a group of modular enzymes widespread in all life Domains. *Synechocystis* sp. PCC 6803 has four FDPs (Flv1-4) essential for photoprotection of photosynthesis. A direct comparison of the Mehler-like reaction (O_2 photoreduction) in high Ci (3% CO_2, HC) and low Ci (air level CO_2, LC) acclimated cells demonstrated that the Flv1/Flv3 heterodimer is responsible for an efficient steady-state O_2 photoreduction under HC, with *flv2* and *flv4* expression strongly down-regulated. Conversely, under LC conditions Flv1/Flv3 acts only as a transient electron sink due to competing withdrawal of electrons by the highly induced NDH-1 complex. Further, *in vivo* evidence is provided indicating that Flv2/Flv4 contributes to the Mehler-like reaction when naturally expressed under LC conditions, or when artificially overexpressed under HC. The O_2 photoreduction driven by Flv2/Flv4 occurs down-stream of PSI in a coordinated manner with Flv1/Flv3 and supports slow and steady-state O_2 photoreduction.

Introduction

A-type flavodiiron proteins (Flvs or FDPs) were originally identified in strict and facultative anaerobes among Bacteria, Archaea and Protozoa and were considered to function in O_2 and/or NO detoxification (Wasserfallen et al., 1998; Gonçalves et al., 2011; Folgosa et al., 2018). All FDPs share two conserved structural domains: the N-terminal metallo-β-lactamase-like domain, harboring a non-heme diiron center, where O_2 and/or NO reduction takes place; and the C-terminal flavodoxin-like domain, containing a flavin mononucleotide (FMN) moiety. The structures of FDPs in anaerobic prokaryotes and eukaryotic protozoa have been resolved as homooligomers (dimer or tetramer comprised of two dimers) arranged in a "head-to-tail" configuration, so that the diiron center of one monomer and the FMN of the other monomer are in close proximity to each other, which ensures rapid electron transfer between the two cofactors.

C-type FDPs, specific to oxygenic photosynthetic organisms, hold an additional flavin-reductase-like domain, coupled with extra cofactors (Romão et al., 2016; Folgosa et al., 2018). *Synechocystis* sp. PCC 6803 (hereafter, *Synechocystis*) possesses four genes encoding FDPs: *sll1521* (Flv1), *sll0219* (Flv2), *sll0550* (Flv3) and *sll0217* (Flv4). Recently resolved crystal structure of truncated Flv1 from *Synechocystis* revealed a monomeric form with a 'bent' configuration (Borges et al. 2019). Photosynthetic FDPs gained attention first in 2002 when recombinant *Synechocystis* Flv3 protein was shown to function in O_2 reduction to water without producing ROS (Vicente et al., 2002). Later it was demonstrated that *Synechocystis* Flv1 and Flv3 proteins function *in vivo* in the photoreduction of O_2 downstream to PSI (Helman et al., 2003). Since then, extensive research has been pursued to reveal the crucial function of Flv1 and Flv3

(and their homologs, FLVA and FLVB in other photosynthetic organisms) as a powerful sink of excess photosynthetic electrons which safeguards PSI and secures the survival of oxygenic photosynthetic organisms under fluctuating light (Allahverdiyeva et al., 2013; Gerotto et al., 2016; Chaux et al., 2017; Jokel et al., 2018) or under the repetitive short-saturation pulses (Shimakawa et al., 2017). The Flv1- and Flv3-mediated alternative electron transport to O_2 was named as the Mehler-like reaction, being a widespread pathway, operating in all photosynthetic organisms from cyanobacteria up to gymnosperms, but lost in angiosperms (Allahverdiyeva et al., 2015; Ilík et al., 2017).

The Flv2 and Flv4 proteins are encoded by an operon together with a small membrane protein, Sll0218. The *flv4-sll0218-flv2* (hereafter *flv4-2*) operon is strongly induced in low Ci (atmospheric 0.04% CO_2 in air, LC) and high light conditions (Zhang et al., 2009). The operon structure is highly conserved in the genome of many *β*-cyanobacteria (Zhang et al., 2012; Bersanini et al., 2014). The *flv4-2* operon-encoded proteins have been reported to function in photoprotection of Photosystem (PS) II, by acting as an electron sink presumably transporting electrons from PSII or plastoquinone (PQ) pool to an unknown acceptor (Zhang et al., 2009, 2012; Bersanini et al., 2014; Chukhutsina et al., 2015). Since *flv2*, *sll0218* and *flv4* are co-transcribed, the contribution of each single protein of the operon to PSII photoprotection has been difficult to dissect. Recent data examining distinct and specific roles of the Flv2/Flv4 heterodimer and the Sll0218 protein (using a set of different mutants deficient only in Sll0218 or in Flv2 and Flv4) demonstrated that the majority of observed PSII phenotypes were actually due to the absence of Sll0218, thus leading to the conclusion that Sll0218 contributes to PSII repair and stability (Bersanini et al., 2017). However,

the exact donor and acceptor of the Flv2 and Flv4 proteins *in vivo* have not been identified and possible cross-talks between all four FDPs have not been established so far, thus limiting our understanding of the function of FDPs on cellular level.

In order to shed light on *in vivo* function of Flv2 and Flv4 and to untangle the function of Flv1/Flv3 from the one of Flv2/Flv4 heterooligomer, we used here a specific set of FDP mutants. The set included: (i) the Δ*flv1*/Δ*flv3* mutant deficient in both Flv1 and Flv3 proteins (Allahverdiyeva et al., 2011); (ii) the Δ*flv2* mutant, which does not express the Flv2 protein, but retains a low amount of Flv4 and the WT level of Sll0218 (Zhang et al., 2012); (iii) the Δ*flv4* mutant which is deficient in the accumulation of three *flv4-2* operon proteins (Zhang et al., 2012); (iv) Δ*sll0218*, which lacks the small Sll0218 protein, but expresses the Flv2 and Flv4 proteins (Bersanini et al., 2017); (v) Δ*flv3*/Δ*flv4*, which represents a deficiency in all four FDPs, whereby the absence of Flv3 results in a strong decrease in Flv1 (Mustila et al., 2016) and the inactivation of Δ*flv4* affects the expression of the whole *flv4-2* operon (Zhang et al., 2012); and finally (vi) the *flv4-2* operon overexpression strain, *flv4-2*/OE, expressing high amounts of Flv2, Flv4 and Sll0218 (Bersanini et al., 2014).

Here, we provide *in vivo* evidence for Flv2/Flv4 mediated O_2 photoreduction in *Synechocystis*. Unlike the rapidly responding powerful Flv1 and Flv3, the more slowly functioning Flv2 and Flv4 proteins are dispensable for survival under fluctuating light intensities. The expression of *flv4* and *flv2* under LC was found to be regulated by pH of the growth media, with significant downregulation observed under strong alkaline pH conditions. Results from this study provide important insights into the response of

photosynthetic organisms to changes in Ci and into how they regulate the availability of electron sinks.

Results

1. Extent and kinetics of the Mehler-like reaction in cells acclimated to low (LC) and high Ci (HC) conditions

Application of membrane inlet mass spectrometry (MIMS) with ^{18}O-enriched oxygen allows differentiation between photosynthetic gross O_2 production and O_2 uptake under illumination. The *flv4-2/*OE cells, accumulating high amounts of Flv2, Sll0218 and Flv4 both in LC and high Ci (> 1% CO_2 in air, HC) conditions (Bersanini et al., 2014), demonstrated substantially higher O_2 photoreduction rates compared to the respective WT (Figure 1A, 1B, 1D). The Flv3 protein level was similar in *flv4-2/*OE and wild-type (WT) cells grown both at LC and HC (Figure 1C) thus strongly supporting the contribution of the *flv4-2* operon proteins to O_2 photoreduction *in vivo* during illumination.

As reported earlier, the Ci level has a remarkable effect on the expression of FDPs at transcript and protein level: Flv2, Flv4 and Flv3 have been strongly upregulated under LC (Zhang et al., 2009; Wang et al., 2004; Battchikova et al., 2010), and down-regulated upon a shift to HC (Zhang et al., 2009; Hackenberg et al., 2012; Figure 1C). Nevertheless, a direct comparison of the efficiency and kinetics of the Mehler-like reaction in HC- and LC-acclimated cells has not been reported, thus making the contribution of different FDPs to O_2 photoreduction difficult to assess. Therefore, as an initial experiment, we evaluated the activity of the Mehler-like reaction in *Synechocystis* cells grown at LC and HC (3% CO_2) conditions, at pH 8.2.

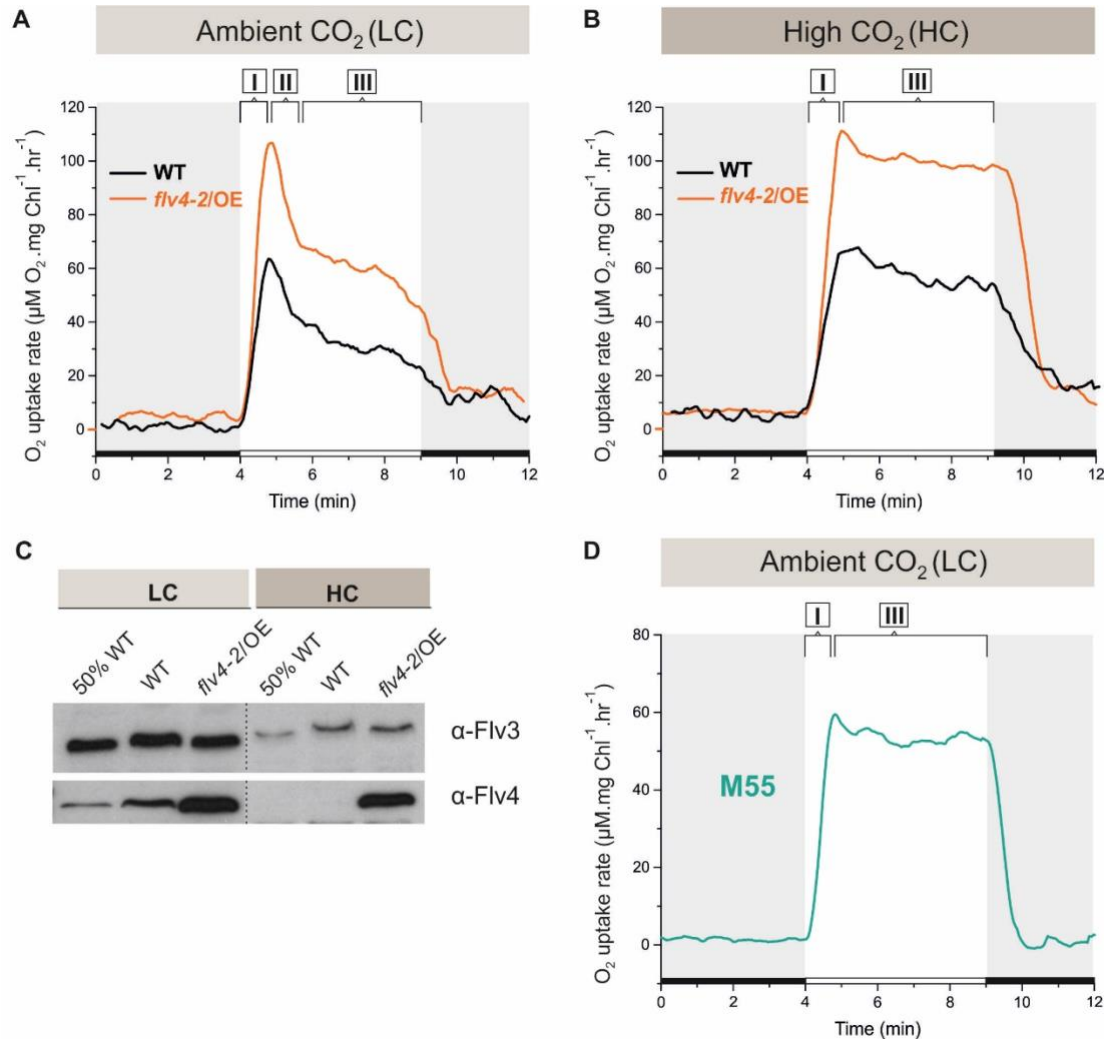

Figure 1. O_2 reduction rates and Flv3 and Flv4 protein accumulation in cells grown in low (LC) and high CO_2 (HC). (A, B) O_2 reduction rate of WT, *flv4-2/*OE and (D) the M55 mutant (Δ*ndhB)* was recorded in darkness (grey background) and under illumination (white background). The experiment was conducted in 3 independent biological replicates and a representative plot is shown. (Figure 1-source data 1). (C) Immunoblot detection of Flv3 and Flv4 in WT and *flv4-2/*OE. Pre-cultures were grown in BG-11, pH 8.2 under 3% CO_2 (HC) for 3 days, after that cells were harvested and resuspended in fresh BG-11, pH 8.2 at OD_{750}=0.2. The experimental cultures were grown under HC or under LC. For the MIMS experiments the cells were harvested and resuspended in fresh BG-11, pH 8.2 at 10 µg Chl *a* mL^{-1}. O_2 photoreduction was recorded during the transition from darkness to high-

light intensity of 500 µmol photons $m^{-2}s^{-1}$. Different phases of O_2 photoreduction kinetics are indicated as {I}, {II}, {III}.

The following source data and figure supplements are available for Figure 1:

Source data 1. O_2 reduction rates of WT, flv4-2/OE and the M55 mutant grown under different CO_2 levels.

Figure supplement 1. *O_2 reduction rates under high CO_2.*

After a shift from darkness, WT cells demonstrated rapid induction of light-induced O_2 uptake both at LC and at HC conditions (59 ± 6.4 and 56 ± 6.4 µmol O_2 mg Chl *a* $^{-1}$ h^{-1}, respectively). This fast induction phase is designated as {I} in Figure 1A and 1B. Yet, the kinetics of O_2 photoreduction in LC-grown cells differed from those grown under HC. In the LC-grown WT cells, the fast induction phase {I} was followed by a clear biphasic quenching of O_2 reduction, namely by the strong decay phase {II}, which continued about a minute, followed by a quasi-stable state, phase {III} (~33 ± 5.9 µmol O_2 mg Chl *a* $^{-1}$ h^{-1}) during illumination. On the contrary, in HC-grown WT cell, the light-induced O_2 reduction rate achieved in the phase {I} declined only slightly during the first 2-3 minutes (from ~ 56 ± 7.7 to ~ 48 ± 6.3 µmol O_2 mg Chl *a* $^{-1}$ h^{-1}). Thereafter it remained nearly at the same rate for at least 5 min (Figure 1B) of illumination. In *flv4-2/*OE cells, grown both in LC- and HC, light-induced O_2 reduction was stronger that in WT. Nevertheless, the kinetic phases of O_2 photoreduction in *flv4-2/*OE cells resembled those of respective WT cells, being relatively stable at HC and demonstrating a strong biphasic quenching at LC.

The Δ*flv2* and Δ*flv4* mutants grown under HC conditions demonstrated a similar O_2 photoreduction pattern as WT, whereas the Δ*flv3*/Δ*flv4* and Δ*flv1*/Δ*flv3* mutants showed hardly any light-induced O_2 reduction (Figure 1- Figure supplement 1). A negligible amount of Flv2 and Flv4 proteins in the WT cells grown at HC (Zhang et al., 2009, 2012; Figure 1C) explains the lack of contribution of these proteins to the Mehler-like reaction and confirms that the Flv1 and Flv3 proteins are responsible for the Mehler-like reaction under HC condition (Helman et al., 2003).

To disclose the reason for the fast decay of O_2 photoreduction observed under LC conditions (Figure 1A), we first tested the putative competition between the NAD(P)H:quinone oxidoreductase (NDH-1) complex and FDPs for available photosynthetic electrons. The NDH-1 complex is a powerful machinery utilizing electrons for cyclic electron transport (CET) around PSI, CO_2 uptake and respiration under LC conditions (Zhang et al., 2004, Schuller et al.., 2019). To this end, the O_2 photoreduction was measured in the M55 mutant (Δ*ndhB*) deficient in the hydrophobic NdhB subunit (Ogawa et al., 1991) and thus lacking all NDH-1 complexes (Zhang et al., 2004). The M55 mutant demonstrated steady-state O_2 photoreduction kinetics during the dark-to-light transition (Figure 1D), resembling in this respect the HC-grown WT cells (Figure 1B; Figure 1- Figure supplement 1) and thus confirming the possible competition for electrons between the NDH-1 complexes and FDPs under LC conditions.

2. Extent and kinetics of the Mehler-like reaction is strongly dependent on pH and the carbonate concentration of the growth medium

Next, the pH and the presence of carbonate in the growth medium were addressed as possible modulators of the extent and kinetics of the Mehler-like reaction and the accumulation of FDPs under LC conditions.

The effect of pH. The WT cells grown at pH 9 demonstrated a strong but only transient Mehler-like reaction: the O_2 photoreduction rate reached its maximum during the first 30 s upon illumination, then quickly declined to the initial level of dark O_2 uptake rate within 1 min of illumination (Figure 2, right panel). Similar to WT, the Δ*flv4* mutant cells demonstrated only a transient O_2 photoreduction upon illumination. No significant O_2 photoreduction could be recorded in the Δ*flv1*/Δ*flv3* and Δ*flv3*/Δ*flv4* mutants grown at pH 9.

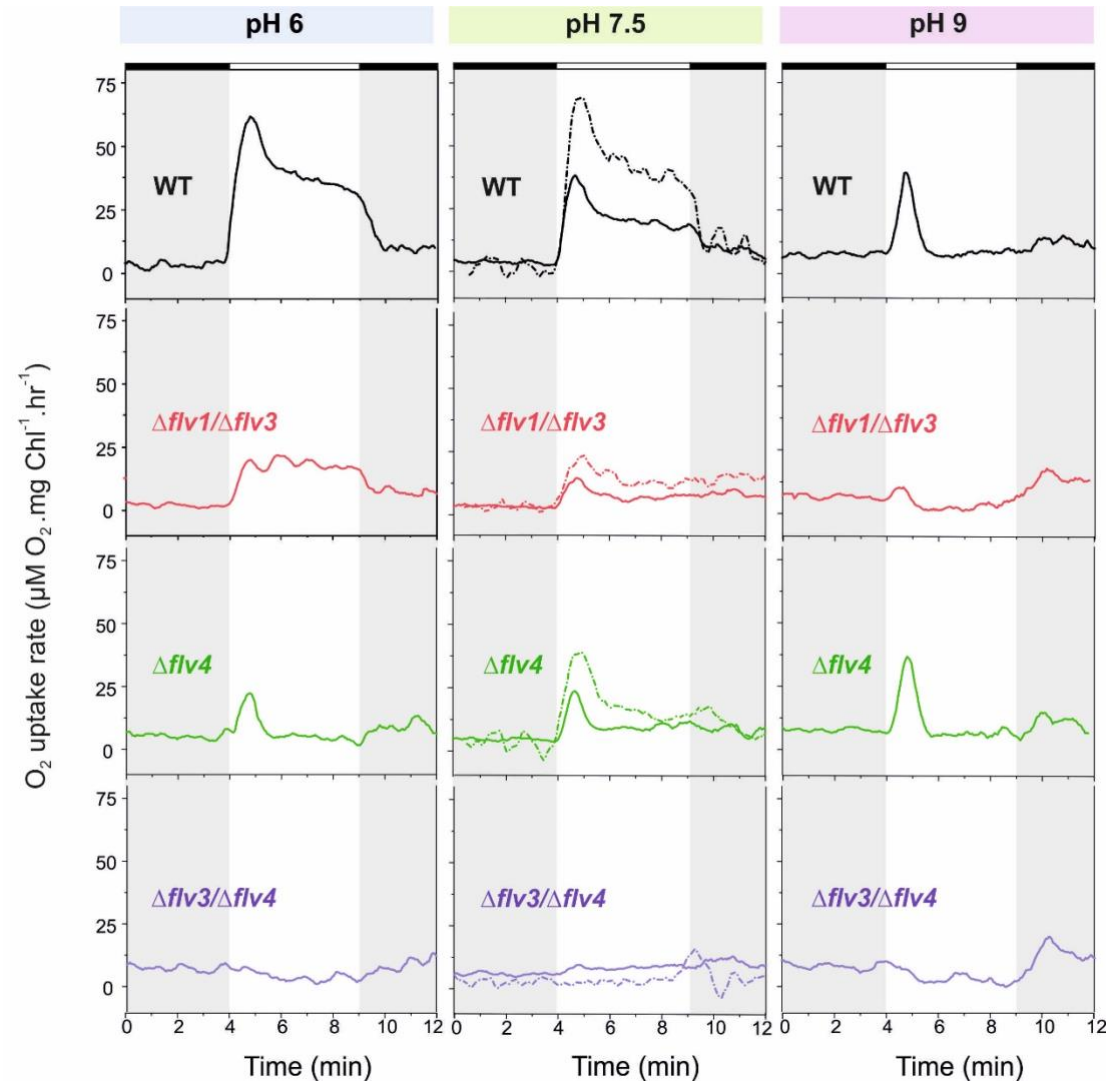

Figure 2. O_2 reduction rates of WT and FDP mutants grown at different pH levels. O_2 reduction rate was recorded in darkness (grey background) and under illumination with actinic white light at an intensity of 500 µmol photons m^{-2} s^{-1} (white background). Pre-cultures were grown under HC for 3 days at different pH levels. For MIMS experiments, cells were shifted to LC at OD_{750}≈0.2 (same pH) and grown for 4 days. Exceptions were: (i) pH 6 experimental cultures were inoculated from pH 8.2 pre-cultures; and (ii) pH 7.5 pre-culture was shifted to LC in BG11, both with and without sodium carbonate (dotted line '- Na_2CO_3') The experiment was conducted in 3 independent biological replicates (except experiment at pH 6 with n= 2 independent biological replicates) and a representative plot is shown. (Figure 2-Source data 1). In order to create comparable conditions for MIMS measurements, all cells were supplemented with 1.5 mM $NaHCO_3$ prior to the measurements. Independent experiments

performed on WT cells grown in the absence of Na_2CO_3, but supplied with 1.5 mM $NaHCO_3$ prior to MIMS measurement showed no significant difference in O_2 photoreduction rates (Figure 2- Figure supplement 1).

The following source data and figure supplement are available for Figure 2:

Source data 1. O_2 reduction rates of WT and FDP mutants grown at different pH levels.

Figure supplement 1. *O_2 photoreduction rates during the dark-to-light transition of WT cells with and without addition of 1.5 mM $NaHCO_3$ prior MIMS measurements.*

Figure supplement 2. *O_2 photoreduction rates of the Δ*flv2* and Δ*sll0218* mutants grown at LC pH 7.5* and 8.2 *with and without Na_2CO_3.*

Immunoblotting using specific antibodies showed that, similarly to the WT cells grown under HC (Figure 1D), the Flv2 and Flv4 proteins were almost undetectable in WT grown under LC at pH 9 (Figure. 3A).

In line with protein data, the transcript levels of both *flv2* and *flv4* were significantly down-regulated in the cells grown at pH 9 (Figure 3B), suggesting a pH-dependent transcriptional regulation of the *flv4* and *flv2*. This is consistent with earlier transcriptional profiling experiments reporting downregulation of *flv2* and *flv4* transcripts after transferring *Synechocystis* from pH 7.5 to pH 10 (Summerfield and Sherman, 2008). Importantly, the accumulation of Flv3 was not affected at pH 9. These results strongly suggest that the conspicuous but transient O_2 photoreduction observed in the WT and Δ*flv4* mutant cells at pH 9 originates mainly from the activity of Flv1/Flv3 heterodimer.

The WT cells grown at pH 6, at pH 7.5 (Figure 2, left and middle panels, respectively) and at pH 8.2 (Figure 1A) demonstrated a rapid induction of O_2 reduction (phase {I}) followed by biphasic decay during illumination: a fast decay phase (phase {II}) and a quasi-stable phase (phase {III}) (Figure 1A and 2). The highest O_2 photoreduction rate was observed in the WT cells grown at pH 6 (Figure 2).

Importantly, the Δ*flv1*/Δ*flv3* mutant also showed residual O_2 photoreduction: only a small O_2 uptake was noticeable at pH 7.5, whereas at pH 6 the O_2 photoreduction rate was substantial and constant during 5 min of illumination of Δ*flv1*/Δ*flv3* (Figure 2). Unlike the Δ*flv1*/Δ*flv3* mutant, both the Δ*flv2* (Figure 2- Figure supplement 2) and Δ*flv4* (Figure 2) mutants showed a strong transient O_2 photoreduction phase, peaking around the first 30 s of illumination and quickly decaying. This occurred at all tested pH levels. These results together with the ones that demonstrated highly increased rates of O_2 photoreduction in the overexpression *flv4-2*/OE strain (Figure 1B) collectively confirmed the *in vivo* involvement of both the Flv2 and Flv4 proteins in O_2 photoreduction. The O_2 photoreduction kinetics of the Δ*sll0218* mutant resembled that of the WT (Figure 1- Figure supplement 1 and Figure 2- Figure supplement 2), thus implying that the Sll0218 protein does not contribute to the Mehler-like reaction under the HC and LC conditions studied here. These results made us to exclude the Δ*sll0218* mutant from any further experiments presented in this section.

The data presented above allowed making preliminary conclusions to be made about the origin of the different kinetic phases of O_2 photoreduction. Since a transient O_2 photoreduction was characteristic for the WT, Δ*flv2* and Δ*flv4* cells, but hardly detectable in Δ*flv1*/Δ*flv3*, it is conceivable that the Flv1/Flv3 heterodimer is mostly

responsible for the strong and transient O_2 uptake during dark-light transitions, whilst Flv2/Flv4 contribute to the steady-state O_2 photoreduction at LC (see Δ*flv1*/Δ*flv3* particularly at pH 6, Figure. 2). The complete lack of O_2 photoreduction in the Δ*flv3*/Δ*flv4* mutant (representing deficiency of all four FDPs) is in line with this hypothesis.

Yet the overall complexity of obtained results called for further investigation. Since not only the FDPs but also distinct variants of the NDH-1 complex as well as HCO_3^- transporters (Zhang et al, 2004) are known to respond to the CO_2 and pH levels of the growth medium, we next evaluated by immunoblotting the abundances of NdhD3, representing a low Ci inducible NDH-1MS complex, and SbtA, a high-affinity low Ci inducible Na^+/HCO_3^- transporter, in WT and different mutants under conditions used for the MIMS experiments.

As expected, in WT cells grown at pH 7.5, NdhD3 and SbtA were not detected under HC conditions, but both proteins were strongly accumulated in LC (Figure 3*D*). However, in LC conditions, the increase in alkalinity of the growth medium to pH 9.0 resulted in markedly lower levels of NdhD3 and SbtA accumulation compared to those observed at pH 7.5. The effect was more pronounced in the case of SbtA. Interestingly, the Δ*flv2* and Δ*flv4* mutants demonstrated the decrease of SbtA accumulation compared to WT even at pH 7.5 in LC, whereas in *flv4/OE* SbtA remained at the same level as in WT (Figure 3D).

Thus, the expression of the SbtA protein closely followed the alterations in the expression of Flv2 and Flv4 proteins under all growth conditions, suggesting that

Flv2/Flv4 and the Ci uptake mechanisms, particularly the inducible high-affinity Na^+/HCO_3^- transporter, share a common regulatory pathway of protein expression.

Unlike the growth media at pH 6 - 8.2, the Ci-pool at pH 9 contains an additional species, CO_3^{2-}. It is possible that a small amount of CO_3^{2-} in the external growth medium acts as a signal to trigger the regulation of *flv2* and *flv4* expression via antisense RNA *as1-flv4* and the master transcription factors, *ndhR* or *cmpR* (Eisenhut et al., 2012). Considering that the double negative charge of CO_3^{2-} prevents its diffusion through the cell membrane, and an active carbonate uptake transporter remains at present unknown, we cannot yet consider CO_3^{2-} as an internal sensor. To get further insights into the carbonate effect on O_2 photoreduction, the MIMS experiments were monitored on FDP mutants grown in the BG-11 medium in the presence and absence of sodium carbonate.

The effect of sodium carbonate. In order to control the available C_i species, the experimental cultures were grown in BG-11 media (pH 7.5) without sodium carbonate (Na_2CO_3). Culturing the cells without Na_2CO_3 at pH 7.5 clearly enhanced O_2 photoreduction in the WT and all studied FDP mutants (Figure 2, middle panel). Despite such a clear variation in O_2 photoreduction rates in WT, no significant difference in gene transcript (Figure 3B) and protein levels (Figure 3C) of FDPs were observed in the presence or absence of Na_2CO_3.

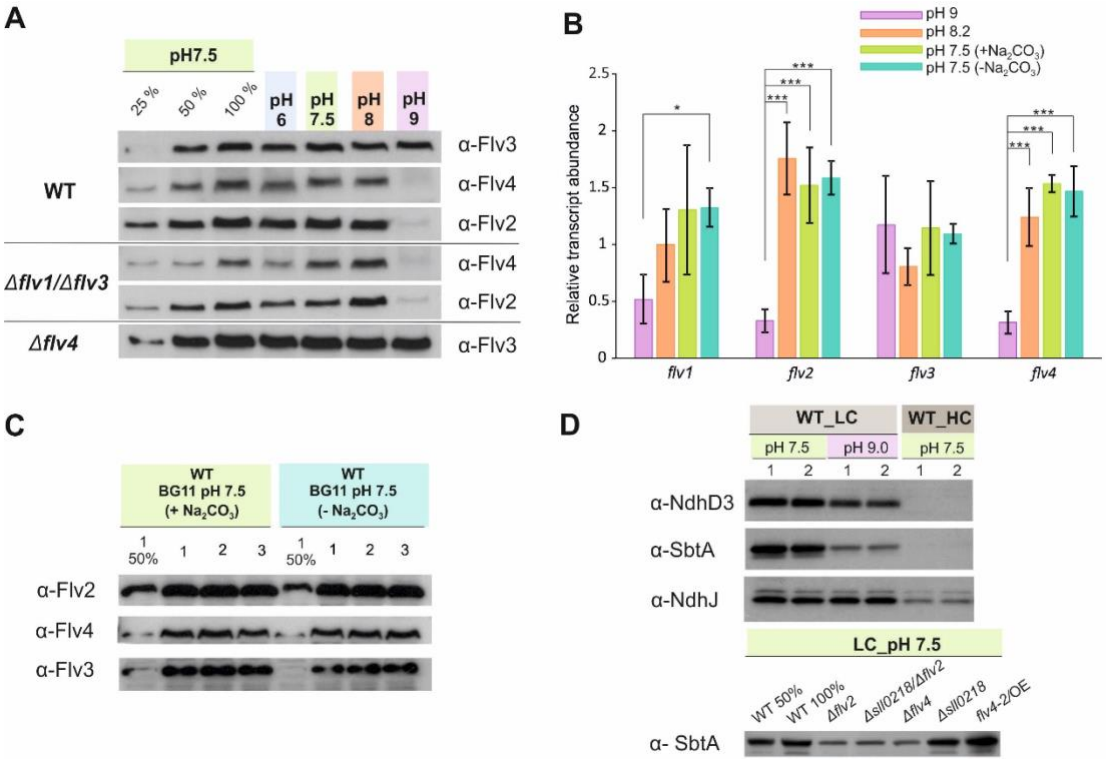

Figure 3. The effect of the pH of growth medium on the protein and transcript accumulation. (A, B) The effect of the pH and (B, C) absence of carbonate in the growth medium (A, C) on the protein and (B) transcript levels of FDP. (D) Protein immunoblots demonstrating the accumulation of bicarbonate transporter (SbtA) and NDH-1 subunits (NdhD3 and NdhJ) in the cells grown at different pH and CO_2 concentration. Cells were pre-grown at different pH levels (+Na_2CO_3) under HC for 3 days, harvested, resuspended in fresh BG-11 (pH maintained), adjusted to OD_{750}≈0.2 and shifted to LC for 4 days. At pH 7.5, the cells were grown at LC in the presence (+ Na_2CO_3) or in the absence (- Na_2CO_3) of sodium carbonate (B, C). Transcript abundance is presented as mean ± SD, n = 2-4 biological replicates, asterisks indicate a statistically significant difference to the WT (*P < 0.05; ***P <0.001) (Figure 3-source data 1). Numbers 1-3 indicate different biological replicates.

The following source data and figure supplement are available for Figure 3:

Source data 1. Transcript abundance of *flv1, flv2, flv3* and *flv4* genes

Figure supplement 1. *O_2 uptake in the WT, flv4-2/OE, Δflv4 and Δcyd mutant.*

3. The FDP induced O_2 photoreduction does not occur at PSII or the PQ-pool level

In order to establish where the Flv2/Flv4 heterodimer related O_2 photoreduction occurs in the electron transport chain we focused on the *flv4-2*/OE mutant (grown at LC, pH 7.5, without carbonate), which showed significantly high accumulation of Flv2 and Flv4 proteins and higher O_2 photoreduction rate than the WT (Figure 1). When linear electron transport was blocked at Cytochrome b_6f (Cyt b_6f) level using DBMIB as an inhibitor (Draber et al., 1970; Yan et al., 2006), both the WT (Ermakova et al., 2016) and *flv4-2*/OE mutant cells demonstrated a strong light-induced O_2 uptake (Figure 3-Figure supplement 1). As expected, in the Δ*cyd* mutant the light-induced O_2 uptake was not detected in the presence of DBMIB (Ermakova et al., 2016). The addition of HQNO, an inhibitor of Cytochrome *bd* quinol oxidase (Cyd), to the DBMIB-treated WT and *flv4-2*/OE completely eliminated O_2 photoreduction. These results confirmed that Cyd was solely responsible for the observed O_2 photoreduction occurring at the PQ-pool level.

4. Growth phenotype of FDP deletion mutants under fluctuating light intensities.

We have previously demonstrated that the Flv1/Flv3 heterodimer enables cell growth under fluctuating light, by functioning in the Mehler-like reaction as an efficient electron sink (Allahverdiyeva et al., 2013). However, the results of the current study clearly suggest an additional involvement of the Flv2/Flv4 heterodimer in the Mehler-like reaction, particularly under conditions of LC and at pH values of 8.2 or lower (Figure 1 and 2). These findings led us to more precisely examine the combined effects of the pH of the growth medium and the fluctuating growth light conditions (FL) on

the growth performance of various FDP mutants. To this end, both severe (FL20/500, when 20 µmol photons m^{-2} s^{-1} background light was interrupted every 5 min by 30 s light pulse intensity of 500 µmol photons m^{-2} s^{-1}) and mild (FL50/500, when 50 µmol photons m^{-2} s^{-1} background light was interrupted every 5 min by 30 s light pulse intensity of 500 µmol photons m^{-2} s^{-1}) fluctuating lights at different pH values of the growth medium were applied. In line with our previous work, the Δ*flv1*/Δ*flv3* mutant (also Δ*flv3*/Δ*flv4*) failed to grow under severe (FL20/500) light fluctuations independently of the pH of the growth medium (Figure 4; Figure 4- Figure supplement 1). Differently to the severe FL20/500 condition, under mild fluctuating light (FL50/500) the Δ*flv1*/Δ*flv3* mutant demonstrated slower growth than WT at alkaline pH of 9 (Figure. 4), and at pH 8.2 (Mustila et al., 2016, Figure 4- Figure supplement 1) and similar growth to the WT at the lower pH 7.5 (Mustila et al., 2016, Figure 4- Figure supplement 1) and pH 6 (Figure 4). Importantly, the Δ*flv4* mutant grew similarly to the WT at all studied pH levels, both under mild and severe FL conditions (Figure 4). The Δ*flv2*, Δ*sll0218* and *flv4-2/OE* mutants also demonstrated similar growth to the WT under severe FL20/500 at pH 7.5 and 8.2 (Figure 4- Figure supplement 1).

The results above strongly suggest that, in contrast to the Flv1/Flv3-originated Mehler-like reaction, the Flv2/Flv4-driven O_2 photoreduction is not essential for the survival of cells under fluctuating light.

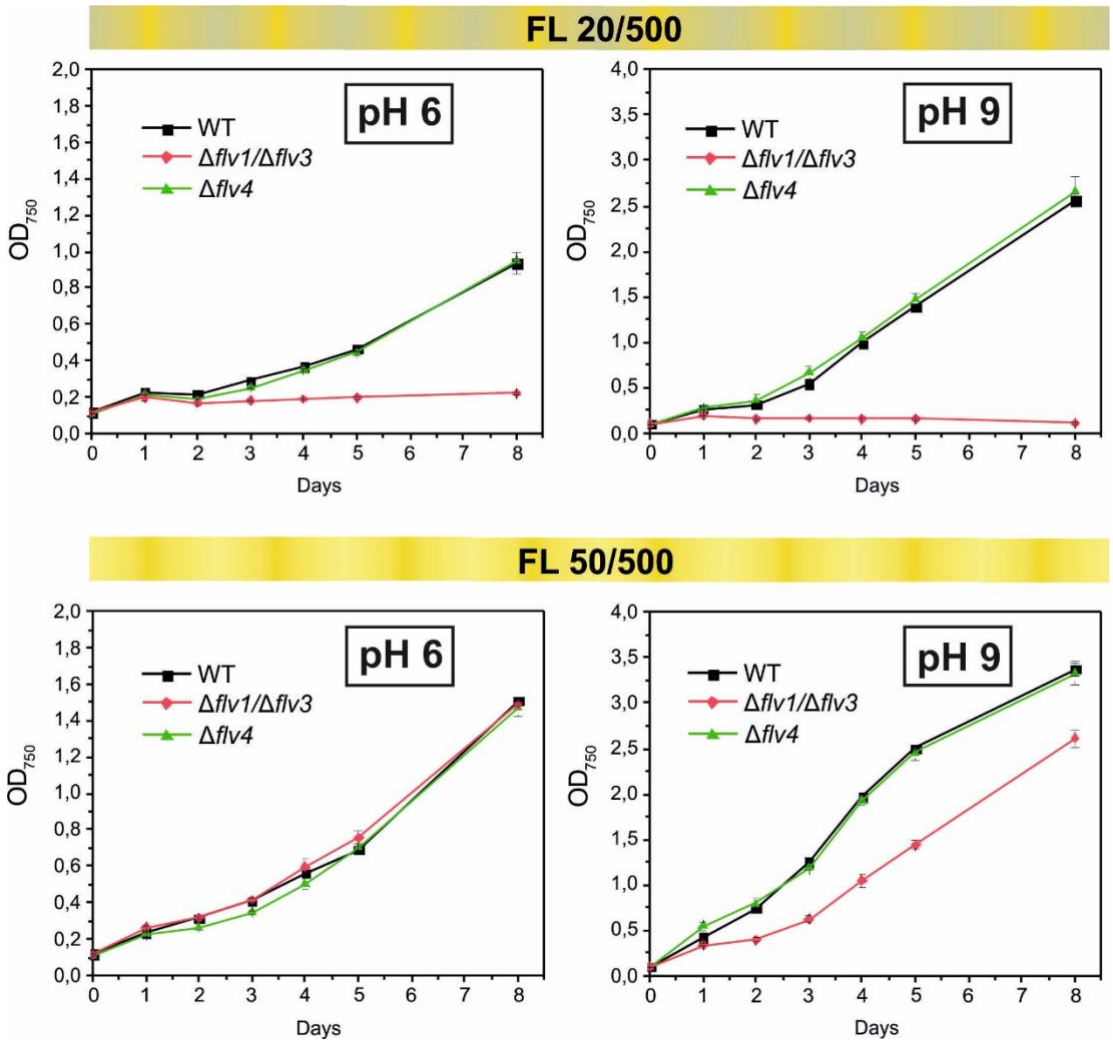

Figure 4. Growth curves of the different FDPs mutants under fluctuating light intensities. Pre-cultures were grown under HC for 3 days illuminated with constant light of 50 µmol photons m^{-2} s^{-1}. The cells pre-grown at pH 9 or pH 8.2 (for experimental culture at pH 6) were harvested, resuspended in fresh BG-11 (pH 9 or 6), adjusted to OD_{750}=0.1 and shifted to LC. Experimental cultures were grown under FL 20/500 or 50/500 regime for 8 days. The experiment was conducted in 2 independent biological replicates and average values was plotted.

The following source data and figure supplements are available for Figure 4:

Source data 1. Growth of the different FDPs mutants under fluctuating light intensities

Figure supplement 1. *Growth curves of the different Flv mutants under fluctuating light intensities*

5. Effect of increasing light intensities on the Mehler-like reaction

In order to assess the response of the Mehler-like reaction to different light intensities, the WT, Δ*flv4* and Δ*flv1*/Δ*flv3* mutant cells were illuminated with 500, 1000 and 1500 μmol photons m^{-2} s^{-1} white light (Figure 5). Increasing light intensity from 500 to 1000 μmol photons m^{-2} s^{-1} resulted in two-fold enhancement of the maximum O_2 photoreduction rate in WT (Figure 5A, 5D). Further increase in light intensity (1500 μmol photons m^{-2} s^{-1}) enhanced only slightly (up to 2.3-fold) the maximum O_2 photoreduction rate, suggesting that the applied light intensity was already saturating. Likewise, the Δ*flv4* mutant demonstrated about 1.9- and 2.3-fold enhancement in the maximum rate of transient light-induced O_2 reduction under 1000 and 1500 μmol photons m^{-2} s^{-1} illumination, respectively (Figure 5C, 5D). On the contrary, the Δ*flv1*/Δ*flv3* mutant, different from WT and Δ*flv4*, showed slower response to increasing light intensities (1.6- and 1.8-fold enhancement in the maximum rate at 1000 and 1500 μmol photons m^{-2} s^{-1}, respectively) (Figure 5B, 5D). It is important to note that both the Δ*flv4* and Δ*flv1*/Δ*flv3* mutants accumulate nearly the WT level of the Flv3 or Flv4/Flv2 proteins, respectively (Zhang et al., 2009; Mustila et al., 2016).

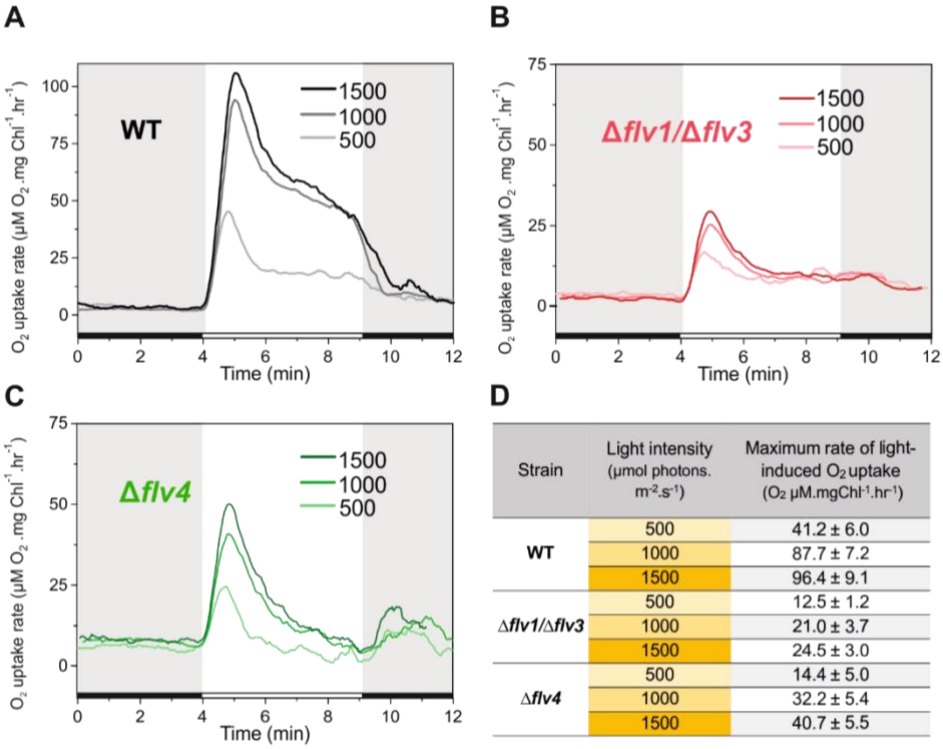

Strain	Light intensity (µmol photons. m-2.s-1)	Maximum rate of light-induced O2 uptake (O2 µM.mgChl-1.hr-1)
WT	500	41.2 ± 6.0
	1000	87.7 ± 7.2
	1500	96.4 ± 9.1
Δflv1/Δflv3	500	12.5 ± 1.2
	1000	21.0 ± 3.7
	1500	24.5 ± 3.0
Δflv4	500	14.4 ± 5.0
	1000	32.2 ± 5.4
	1500	40.7 ± 5.5

Figure 5. Rates of O_2 reduction in response to increasing light intensity in WT, Δ*flv1*/Δ*flv3* and Δ*flv4* mutant cells (A, B, C, respectively). O_2 reduction rate was recorded in darkness (grey background) and under illumination with actinic white light intensities of 500, 1000 and 1500 µmol photons m^{-2} s^{-1} (white background). Pre-cultures were grown under 3% CO_2 (HC) at pH 7.5 for 3 days and then shifted to LC (atmospheric 0.04% CO_2 in air) at OD750=0.2 and pH 7.5 for 4 days. For MIMS measurements, cells were harvested and resuspended in fresh BG11 medium at a Chl *a* concentration of 10 µg mL^{-1}. (D) Maximum rate of light-induced O_2 uptake (O_2 µM. $mgChl^{-1}.hr^{-1}$) of WT, Δ*flv1*/Δ*flv3* and Δ*flv4* mutant cells at different light intensities applied. The experiment was conducted in 3 independent biological replicates and a representative plot is shown (Figure 5-source data 1).

The following source data is available for Figure 5:

Source data 1. Rates of O_2 reduction in response to increasing light intensity in WT, Δ*flv1*/Δ*flv3* and Δ*flv4* mutant cells.

The fast and transient response of the Δ*flv4* mutant cells to drastic increase in the light intensity (Figure 5C) confirmed a high capacity of Flv1/Flv3-related O_2 photoreduction as an electron sink. These results explain the essential role of Flv1/Flv3, unlike Flv2/Flv4, for the survival of cells under fluctuating light intensities. Intriguingly, both the fast induction phase {I}) and quasi-stable phase {III} of O_2 photoreduction rate in WT were notably greater than summation of the individual O_2 photoreduction rates from Δ*flv1*/Δ*flv3* and Δ*flv4*, thus implying a clear enhancement of O_2 photoreduction by various oligomer activities in the presence of all four FDPs.

6. Growth history of cells has long-term consequences on the Mehler-like reaction

The inoculum size (starting OD_{750} value) determines how well the light penetrates into the culture upon starting the cultivation. In previous studies, cells were pre-grown in HC, then harvested at a late logarithmic phase and inoculated in fresh BG-11 (pH 8.2) at OD_{750}≈0.4-0.5, before the shift to LC for the next 3 days (Allahverdiyeva et al., 2011, 2013; Ermakova et al., 2016). To ensure better light penetration to the cultures and to improve the acclimation of cells to the conditions used in this study, the experimental WT and Δ*flv1*/Δ*flv3* cultures were inoculated at a low OD_{750}≈0.1-0.2 and then cultivated for 4 days (instead of 3 days in previous studies). The WT cells grown under LC from a lower OD (OD_{750}≈0.2) demonstrated notably higher O_2 uptake during illumination, compared to the cells shifted to LC at OD_{750}≈0.5 (Figure. 6A). Importantly, the Δ*flv1*/Δ*flv3* mutant cells shifted to LC at a lower OD (OD_{750}≈0.2) also demonstrated a residual steady-state O_2 photoreduction activity.

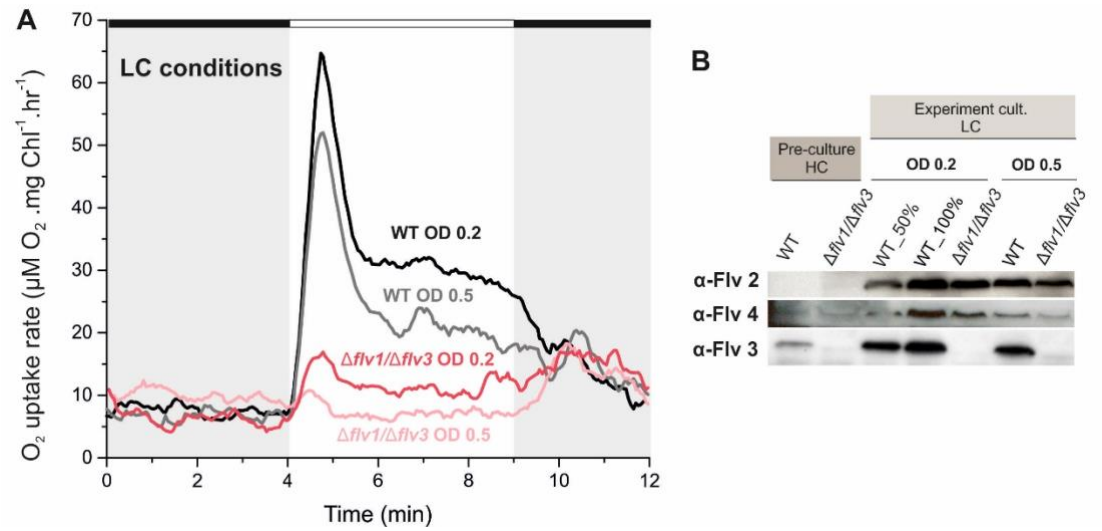

Figure 6. Effect of inoculum size on the O_2 photoreduction and accumulation of FDPs in the WT and Δ*flv1*/Δ*flv3* mutant cells. (*A*) Rates of O_2 uptake measured by MIMS during darkness (grey background) and under illumination with actinic white light at an intensity of 500 µmol photos $m^{-2}s^{-1}$ (white background). (*B*) Protein immunoblots showing the relative accumulation of different FDPs in the WT and Δ*flv1*/Δ*flv3* mutant cells. Pre-cultures were grown in BG-11 (pH 8.2) under HC until late logarithmic phase (OD_{750}≈2.5), then harvested and inoculated in fresh BG-11 under LC at OD_{750}=0.2 for 4 days or OD_{750}=0.5 for 3 days. The experiment was conducted in 3 independent biological replicates and a representative plot is shown in (A).

The following source data is available for Figure 6:

Source data 1. Rates of O_2 reduction of WT, Δ*flv1*/Δ*flv3* and Δ*flv4* mutant cells grown at different inoculum size.

Immunoblot analysis using specific FDP antibodies showed that the WT cells transferred from HC to LC at OD_{750}=0.2 accumulated higher amount of the Flv2, Flv3 and Flv4 proteins compared to the cells shifted to LC at OD_{750}=0.5 (Figure 6B). A similar trend was also observed in the Δ*flv1*/Δ*flv3* mutant, which accumulated more

Flv2 and Flv4 when cultivated at LC from OD_{750}=0.2. This is in line with previous results showing that the accumulation of *flv2* and *flv4* transcripts in *Synechocystis* (upon a shift from HC to LC, Zhang et al., 2009) and vegetative cell-specific *flv1A* and *flv3A* transcripts in *Anabaena* sp. PCC 7120 (upon a shift from dark to light, Ermakova et al., 2013) strongly depended on light intensity.

The results above highlight the long-lasting "memory" of cells for accumulation and activity of FDPs upon a shift of cells from pre-culture conditions to different experimental conditions for assessing the specific roles of the FDPs in O_2 photoreduction.

Discussion

1. The Flv2/Flv4 heterodimer contributes to the Mehler-like reaction when naturally expressed under LC conditions or artificially overexpressed under HC

By characterizing *Synechocystis* mutants specifically affected in the accumulation of various FDPs, we show here that Flv2 and Flv4, together with Flv1 and Flv3 proteins, are involved in O_2 photoreduction *in vivo*. Until recently, it has generally been accepted that the Flv1/Flv3 proteins safeguard PSI under both HC and LC conditions (Allahverdiyeva et al., 2013), whereas proteins, encoded by the *flv4-2* operon and highly expressed under LC, functioning in the photoprotection of PSII by, presumably, directing excess electrons from PSII to an as yet unknown acceptor (Zhang et al., 2009., Zhang et al., 2012; Shimakawa et al., 2015). The possibility of the Flv2/Flv4 contribution to O_2 photoreduction *in vivo* was neglected due to lack of evidence for light-induced O_2 uptake in Δ*flv1* and/or Δ*flv3* mutants (Helman et al., 2003;

Allahverdiyeva et al., 2011; Allahverdiyeva et al., 2013). Thus, Flv1 and Flv3 were assumed to be solely responsible for the Mehler-like reaction. Recently, it was demonstrated that *Synechocystis* Flv4 protein expressed in *E. coli* is capable of NADH-dependent O_2-reduction *in vitro* (Shimakawa et al., 2015). However, the reaction rate was extremely low (almost residual) compared to the activity of FDP from anaerobic bacteria (Di Matteo et al., 2008) and the enzyme showed no affinity to NADPH. Similar scenario was previously presented for the Flv3 protein, where *in vitro* studies performed on recombinant *Synechocystis* protein led to a claim that Flv3 functions as a homodimer in NADH-dependent O_2 reduction (very low affinity to NADPH) (Vicente et al., 2002), whilst subsequent study with Δ*flv1*-OE*flv3* (or Δ*flv3*-OE*flv1*) mutants clearly demonstrated that homooligomers of Flv3 (or Flv1) do not function in O_2 photoreduction *in vivo* (Mustila et al., 2016). Such discrepancies between the *in vitro* and *in vivo* results suggest that the *in vitro* assays conducted thus far have apparently failed to take into full consideration all the complex intracellular interactions, *e.g*. the involvement of Fed or FNR as an electron donor for FDPs, or the *in vitro* experiments do not necessarily demonstrate the processes occurring *in vivo*.

In this study, we provide compelling evidence for the *in vivo* contribution of Flv2/Flv4 to the O_2 photoreduction by applying ^{18}O-labelled-oxygen and real-time gas-exchange measurements to distinct FDP deletion mutants. The inactivation of *flv2* or *flv4* is shown to result in a substantial decrease of O_2 photoreduction in the mutants compared to WT, while the overexpression of the *flv4-2* operon increases the rate of O_2 photoreduction approximately two-fold. In addition, the possibility that the small protein Sll0218 contributes to the Mehler-like reaction is excluded (Figure 1- Figure supplement 1, compare Figure 2- Figure supplement 2 and Figure 2).

It is noteworthy that both the Δ*flv2* (deficient in Flv2 but retaining a low amount of Flv4) and Δ*flv4* (deficient in both Flv2 and Flv4) mutants showed similar inhibition of O_2 photoreduction rates thus supporting the function of Flv2/Flv4 as a heterodimer in the Mehler-like reaction. The existence of the Flv2/Flv4 heterodimer has been proved biochemically in *Synechocystis* (Zhang et al. 2012). Nonetheless, our data do not exclude the possibility that Flv2/Flv2 and/or Flv4/Flv4 homooligomers are involved also in processes other than O_2 photoreduction. Such a situation occurs with the Flv1 and Flv3 proteins, which contribute as homooligomers to the photoprotection of cells under fluctuating light conditions, probably *via* an unknown electron transport and/or regulatory network (Mustila et al., 2016).

The complete elimination of light-induced O_2 reduction in the WT cells grown at pH 8.2 (Ermakova et al., 2016) or at pH 7.5 (Figure 3- Figure supplement 1.) in the presence of electron-transport inhibitors DBMIB and HQNO, blocking photosynthetic electron transport at the level of Cytb_6f and Cyd, respectively, suggests that no FDP-driven O_2 photoreduction (neither by Flv1/Flv3 nor by Flv2/Flv4) does occur at the PSII or PQ-pool level. This conclusion is also supported by the fact that different from WT and the mutants deficient in FDPs, the Δ*cyd* mutant does not exhibit a light induced O_2 uptake in the presence of DBMIB (Ermakova et al., 2016; Figure 3- Figure supplement 1).

The results discussed above clearly indicate that both the Flv1/Flv3 and Flv2/Flv4 heterodimers have a capacity to drive the Mehler-like reaction, functioning downstream of PSI.

2. The Flv1/Flv3 heterodimer drives a strong and steady-state O_2 photoreduction under HC

It is generally accepted that under LC conditions, the slowing down of the Calvin-Benson cycle leads to a build-up of reduced stromal components (Cooley and Vermaas, 2001; Holland et al., 2015), which would stimulate the Mehler reaction to dissipate excess electrons (Ort and Baker, 2002), whilst in HC conditions relatively low electron flux to O_2 via the Mehler reaction is expected. In this study we provide evidence that the HC-grown WT cells are capable of equally high O_2 photoreduction as the respective LC-grown WT cells and of maintaining the steady-state activity at least during the first 5-10 min of illumination (Figure 1A). Compared to WT, a drastically lower O_2 photoreduction rate in the Δ*flv1*/Δ*flv3* and Δ*flv3*/Δ*flv4* mutants grown in HC confirms that O_2 uptake in these conditions is mostly due to Flv1/Flv3-driven Mehler-like reaction (Figure 1- Figure supplement 1).

It is important to note, that the O_2 photoreduction capacity of *Synechocystis* in general correlates with the abundance of the FDPs (Figure 1 and 6). However, the protein abundance is not the only factor that determines the O_2 photoreduction capacity. Indeed, despite the strong and steady-state O_2 photoreduction, the HC-grown cells demonstrate nearly undetectable Flv2 and Flv4 and low amount of Flv3 compared to that under LC. Furthermore, the increase in O_2 photoreduction rate (Figure 2, middle panel) by omitting sodium carbonate from the growth media at pH 7.5, did not correlate with any significant change in the transcript and protein levels of the FDPs, thus suggesting a possible redox regulation of the enzyme activity.

3. The Flv1/Flv3 heterodimer is a rapid, strong and transient electron sink, whereas Flv2/Flv4 supports steady-state O_2 photoreduction under LC

The Mehler-like reaction of WT cells grown under LC at pH 6 - 8.2 exhibits a triphasic kinetics of O_2 photoreduction originating from the activity of both Flv1/Flv3 and Flv2/Flv4 heterodimers (Figure 2). In this study, we were able to unravel the contribution of Flv1/Flv3 and Flv2/Flv4 heterodimers to the O_2 photoreduction kinetics: Flv1/Flv3 is mainly responsible for the rapid transient phase, whereas Flv2/Flv4 is mostly contributing to the slow steady-state phase.

The almost complete absence of Flv2 and Flv4 proteins in WT cells grown under LC at pH 9 provides an excellent model system, where the Mehler-like reaction is naturally driven solely by the Flv1/Flv3 heterodimer, as it is the case also under HC conditions. However, in contrast to HC-grown cells, where Flv1/Flv3 can drive a steady-state O_2 photoreduction, the cells grown under LC at pH 9 demonstrate strong but only transient O_2 photoreduction, which decays during the first 1-2 minutes of illumination (Figure 2). The identical O_2 photoreduction kinetics of the WT cells grown at pH 9 (accumulating Flv3 but lacking both the Flv2 and Flv4 proteins) and the Δ*flv4* mutant (accumulating Flv3 but lacking Flv4 and also Flv2), together with the complete absence of O_2 photoreduction in the Δ*flv3*/Δ*flv4* mutant demonstrate that under LC, the Flv1/Flv3 heterodimer contributes to the Mehler-like reaction in a fast and transient manner (Figure 2). Similar conclusion was previously suggested in *Synechocystis* (Allahverdiyeva et al., 2013) and for the FlvA and FlvB proteins in *Physcomitrella patens* (Gerotto et al., 2016) and *Chlamydomonas reinhardtii* (Chaux et al., 2017; Jokel et al., 2018).

The sole contribution of Flv2/Flv4 to the Mehler-like reaction is clearly demonstrated as a steady-state O_2 photoreduction by the Δ*flv1*/Δ*flv3* mutant grown at LC pH 6 (Figure 2), whilst the same mutant cells grown at pH 7.5 and 8.2 show only residual steady-state O_2 photoreduction. It is important to note that the Flv2/Flv4 heterodimer, when expressed, can readily contribute to O_2 photoreduction under HC as demonstrated by the *flv4-2*/OE strain (Figure 1), thus excluding all redox and structural hindrances for Flv2/Flv4 to function in O_2 photoreduction at HC. However, such contribution is naturally abolished in WT cells grown under high levels of CO_2 by down-regulation of the *flv4-2* operon (Zhang et al., 2009; Zhang et al., 2012).

The rate of the Mehler-like reaction in WT cells exceeds the cumulative O_2 photoreduction driven solely by Flv1/Flv3 (observed in Δ*flv4*) and Flv2/Flv4 (observed in Δ*flv1*/Δ*flv3*). This demonstrates that all the four FDPs are required for an efficient Mehler-like reaction in WT cells upon growth under LC (except at pH 9). A complex interaction between FDPs possibly arises from a coordinated inter-regulation of Flv1/Flv3 and Flv2/Flv4 heterodimers and on possible occurrence of some active Flv1-4 oligomer (Figure 7). Despite detection of homotetrameric organization of *Synechocystis* Flv3 *in vitro* (Mustila et al. 2016), the direct biochemical demonstration of homo- or heterotetramers *in vivo* have not been successful.

The growth inhibition of Δ*flv1*/Δ*flv3* cells under severe fluctuating conditions (FL 20/500) at pH 8.2 (Allahverdiyeva et al., 2013), pH 7.5 (Mustila et al., 2016), pH 6 and pH 9 (Figure 5) demonstrate the essential role of Flv1 and/or Flv3 during drastic changes of light intensity, whereas Flv2 and Flv4 are dispensable under the same conditions (Figure 4, Figure 4- Figure supplement 1). Here, we demonstrate that the

crucial importance of Flv1/Flv3 heterodimers relies on their high capacity to rapidly and effectively respond to increasing light intensities (Figure 5). By adjusting their O_2 photoreduction activity, the Flv1/Flv3 heterodimer works as an efficient and fast sink of electrons, whereas the responsiveness of Flv2/Flv4 is relatively limited and the heterodimer mostly functions at slow time-scale in a steady-state O_2 photoreduction.

The intracellular location of these enzymes may partially contribute to the difference in O_2 photoreduction: Flv1 and Flv3 are soluble cytosolic proteins able to quickly associate with soluble Fed and direct electrons towards O_2 photoreduction. In line with this, the possible interaction between *Synechocystis* Flv1, Flv3 and Fed (Hanke et al., 2011), Flv3 and Fed9 (Cassier-Chauvat and Chauvat, 2014), *Chlamydomonas reinhardtii* FLVB and FED1 (Peden et al., 2013) have been reported. The Flv2/Flv4 heterodimer, specific for cyanobacteria, was suggested to bind to the thylakoid membrane upon increase in Mg^{2+} concentration on the cytoplasmic surface of the thylakoid membrane when the lights are turned on (Zhang et al., 2012). Likely, the association of Flv2/Flv4 with the membrane enhances the electron transfer from Fed (or FNR) to Flv2/Flv4 and would probably result in a delayed and limited O_2 photoreduction activity by Flv2/Flv4. Yet, the possibility that FDPs accept electrons from different and specific Fed paralogs cannot be excluded.

4. Traffic downstream of PSI affects the FDP-mediated Mehler-like reaction

The questions arise as to why Flv1/Flv3 driven O_2 photoreduction is only transient in cells grown under LC and why an extra Flv2/Flv4 pair is required to drive the Mehler-like reaction in *Synechocystis*.

Unlike WT cells demonstrating biphasic decay kinetics of O_2 photoreduction under LC conditions (Figure 1A and Figure 2), the M55 mutant (deficient in CET, CO_2 uptake and respiration) (Ohkawa et al., 2000) shows steady-state O_2 photoreduction, similar to the HC-grown WT (Figure 1B and 1D). This suggests that the strongly upregulated NDH-1 complex under LC in *Synechocystis* (Zhang et al., 2004), contributes to a rapid quenching of O_2-photoreduction (Figure 1A, phase {II}) by efficient withdrawal of electrons from reduced Fed. Under such circumstance, the low but steady-state activity of the Flv2/Flv4 heterodimer is likely to be important for keeping linear electron transport in an oxidized state. This would explain why the PQ-pool is more oxidized in the presence of Flv2/Flv4 and more reduced in its absence, indirectly affecting PSII activity (Zhang et al., 2012; Bersanini et al., 2014 and Chukhutsina et al., 2015). Thus, by allocating the roles of FDPs between the two pairs of heterodimers (Flv1/Flv3 and Flv2/Flv4), the cells are well positioned to respond appropriately to changing C_i levels as well as to abrupt changes in light intensity, in a coordinated and energetically efficient manner.

Unlike prokaryotic cyanobacteria, chlorophytic algae (*e.g. Chlamydomonas reinhardtii*) and mosses rely not only on the FDP-driven pathway, but also harbor the PROTON GRADIENT REGULATION5 (PGR5)/PGR5-LIKE PHOTOSYNTHETIC PHENOTYPE 1 (PGRL1) pathway which operates concomitantly to protect the cells under fluctuating light. It is noteworthy, however, that the PGR5/PGRL1 machinery in *Chlamydomonas reinhardtii* is neither fast nor strong enough to mitigate acceptor-side pressure under highly fluctuating light intensities. To complement this deficiency, the FDP-mediated pathway is indispensable for coping with sudden increases in light intensity (Jokel et al., 2018). Interestingly, the introduction of *Physcomitrella patens*

FDPs rescues a fluctuating light phenotype of the PGR5 *Arabidopsis thaliana* mutant (Yamamoto et al., 2016; 2019), and alleviates PSI photodamage in the PGR5-RNAi, *crr6* (defective in NDH-dependent CET) and the PGR5-RNAi *crr6* double mutants of *Oryza sativa* by acting as a safety valve under fluctuating light and substituting for CET without competing with CO_2 fixation under constant light (Wada et al., 2017). Moreover, the expression of *Synechocystis* Flv1 and Flv3 in tobacco plants enhances photosynthetic efficiency during dark-light transitions by providing an additional electron sink (Gómez et al., 2018). Although data on Flv2/Flv4 proteins expressed in angiosperms is not yet available, our results collectively suggest that the FDP pathway(s) is important to consider in future high-yield crop development and microbial cell factories.

Figure 7 provides a summary scheme of our understanding of the function and interaction of the different FDPs and their oligomers in photoprotection of the photosynthetic apparatus in the model cyanobacterium *Synechocystis* sp. PCC 6803. The importance of the available Ci species in the function and accumulation of FDPs is emphasized by separate schemes for the HC and LC growth conditions.

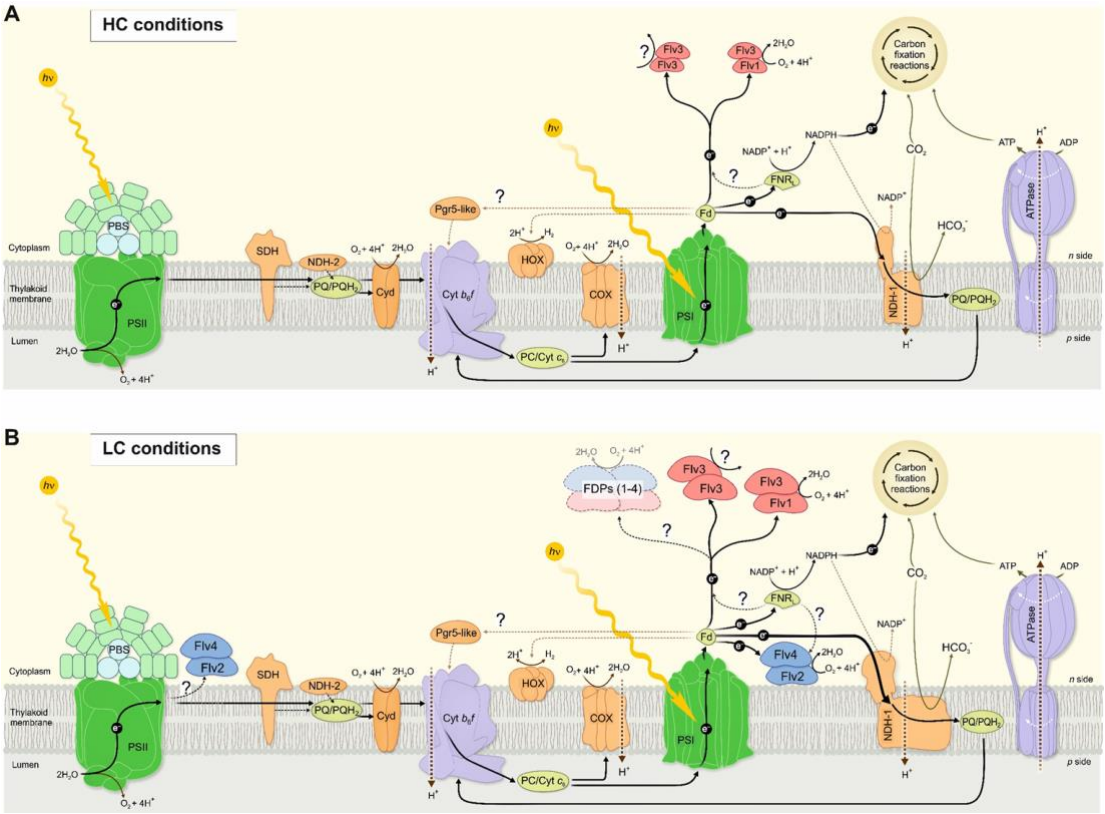

Figure 7. A schematic drawing of photosynthetic light reactions and alternative electron transport routes. (A) A steady-state Mehler-like reaction in HC is carried out by the low-abundant, yet catalytically efficient Flv1/Flv3 heterodimer. The Flv3/Flv3 homooligomer is involved in photoprotection as an electron valve with unknown acceptor or as a component of a signaling/regulating network (Mustila et al., 2016). (B) In LC-grown cells the two pairs of FDP heterodimers are involved in Mehler-like reaction: Flv1/Flv3 mainly drives rapid and transient O_2 photoreduction and Flv2/Flv4 operates relatively slowly and provides a steady-state background O_2 photoreduction. The soluble Flv1/Flv3 heterodimers function as an immediate acceptor of electrons originated from the thylakoid membrane, whereas association of Flv2/Flv4 with the thylakoid membrane (and/or Flv1/Flv3) is controlled by *pmf* and Mg^{2+}. Several oligomeric forms of FDPs are hypothesized to exist, including a heterotetramer comprising different FDP protein compositions. The higher abundance of total NDH-1 complexes and FDPs oligomers in LC conditions, compared to HC conditions, is represented by larger size of the protein complexes.

Materials and Methods

Strains and culture conditions

The glucose-tolerant *Synechocystis* sp. PCC 6803 was used as wild type (WT) strain (Williams, 1988). The FDP inactivation mutants Δ*flv2*, Δ*flv4* (Zhang et al., 2012), and the double mutants Δ*flv1*/Δ*flv3* (Allahverdiyeva et al., 2011), and Δ*flv3*/Δ*flv4* (Helman et al., 2003) have been described previously. The *flv4-2*/OE and Δ*sll0218* mutants were described in (Bersanini et al., 2014; Bersanini et al., 2017).

Pre-experimental cultures were grown at 30°C in BG11 medium, illuminated with continuous white light of 50 µmol photons m^{-2} s^{-1} (growth light: GL), under air enriched with 3% CO_2 (high carbon: HC). BG-11 medium was buffered with 20 mM 2-(N-morpholino) ethanesulfonic acid (MES, pH 6.0), 20 mM HEPES-NaOH (pH 7.5), 10 mM TES-KOH (pH 8.2) or 10 mM N-Cyclohexyl-2-aminoethanesulfonic acid (CHES, pH 9.0), according to the pH of the experimental condition. Pre-cultures were harvested at logarithmic growth phase, inoculated in fresh BG-11 medium at OD_{750}= 0.2 (or OD_{750} = 0.5 when mentioned), measured with and shifted to low CO_2 (atmospheric 0.04% CO_2 in air, LC). OD_{750} was measured using Lambda 25 UV/VIS spectrometer (PerkinElmer, USA). HC experimental cultures were inoculated at OD_{750}= 0.1 and kept at HC for 3 days. During experimental cultivation, cells were grown under continuous GL at 30°C with agitation at 120 rpm and without antibiotics. For growth curves, cells pre-cultivated under continuous GL and HC were collected, inoculated at OD750= 0.1 and shifted to LC under a light regime with a background light of 20 µmol photons m^{-2} s^{-1} interrupted with 500 µmol photons m^{-2} s^{-1} for 30 s every 5 min (FL 20/500) or 50 µmol photons m^{-2} s^{-1} interrupted with 500 µmol photons

m^{-2} s^{-1} for 30s every 5 min (FL 50/500). Sodium carbonate was omitted from the BG-11 ingredients when mentioned.

Absence of contamination with heterotrophic bacteria was checked by dropping liquid culture on LB and R2A agar plates and kept at 30°C.

Isolation of total RNA and Real-time quantitative PCR (RT-qPCR)

Total RNA was isolated from exponentially growing *Synechocystis* by hot-phenol method previously described (Tyystjärvi et al., 2001). After removing any residual genomic DNA, the RNA concentration and purity were measured with a NanoDrop spectrophotometer (Thermo Scientific, USA). RNA integrity was verified by agarose gel electrophoresis.

Complementary DNA was synthesized from 1 µg of purified RNA using the iScript cDNA Synthesis Kit (BioRad, USA) according to the manufacturer's protocol. Synthesized cDNA was diluted four-fold and used as template for the RT-qPCR. The samples for RT-qPCR were labeled by iQ SYBR Green Supermix (BioRad, USA) to detect accumulation of amplicons in 96-well plates. The primers to detect transcripts of *flv1* and *flv2* as well as for the reference genes *rnpB* and *rimM* are described in Mustila et al. 2016. The forward and reverse primers for *flv3* were 5'-CAACTCAATCCCCGCATTAC-3' and 5'-CAGTGGAGATTCGGAGCACT-3' and for *flv4* 5'-ACGATGCCTGGAGTCAAAAC-3' and 5'-GGGTATCCGCCACACTTAGA-3'. The PCR protocol was as follows: 3 min initial denaturation of cDNA at 95˚C, followed by 40 cycles of 95˚C for 10 s, annealing in 57˚C for 30 s and extension in 72˚C for 35 s. A melting curve analysis was performed at the end. Relative changes in the gene expression were determined using the qbase+

software by Biogazelle. One-way ANOVA analysis performed with SigmaPlot was used to determine significant changes in gene expression.

MIMS experiments

In vivo measurements of $^{16}O_2$ (mass 32) and $^{18}O_2$ (mass 36) exchange was performed using a Membrane-inlet mass spectrometry (MIMS) as described previously in (Mustila et al., 2016). Cells were harvested, adjusted to 10 µg Chl *a* mL^{-1} in fresh BG-11 medium and acclimated for 1 h to the same experimental conditions as was applied for the cultivation.

Protein Isolation, electrophoresis and immunodetection

Total cell extracts and the soluble fractions of *Synechocystis* cells were isolated as described (Zhang et al., 2009). Proteins were separated by 12% (w/v) SDS-PAGE containing 6M urea and transferred onto a PVDF membrane (Immobilion-P; Millipore, Germany) and immunodetected by protein specific antibodies.

Competing interests: The authors declare that no competing interests exist.

References

Allahverdiyeva, Y., Mustila, H., Ermakova, M., Bersanini, L., Richaud, P., Ajlani, G., … Aro, E.-M. (2013). Flavodiiron proteins Flv1 and Flv3 enable cyanobacterial growth and photosynthesis under fluctuating light. *Proceedings*

of the National Academy of Sciences, *110*(10), 4111–4116. https://doi.org/10.1073/pnas.1221194110

Allahverdiyeva, Y., Ermakova, M., Eisenhut, M., Zhang, P., Richaud, P., Hagemann, M., … Aro, E. M. (2011). Interplay between flavodiiron proteins and photorespiration in *Synechocystis* sp. PCC 6803. *Journal of Biological Chemistry*, *286*(27), 24007–24014. https://doi.org/10.1074/jbc.M111.223289

Allahverdiyeva, Y., Isojärvi, J., Zhang, P., & Aro, E.-M. (2015). Cyanobacterial Oxygenic Photosynthesis is Protected by Flavodiiron Proteins. *Life*, *5*(1), 716–743. https://doi.org/10.3390/life5010716

Battchikova, N., Vainonen, J. P., Vorontsova, N., Kerãnen, M., Carmel, D., & Aro, E. M. (2010). Dynamic changes in the proteome of *Synechocystis* 6803 in response to CO_2 limitation revealed by quantitative proteomics. *Journal of Proteome Research*, *9*(11), 5896–5912. https://doi.org/10.1021/pr100651w

Bersanini, L., Battchikova, N., Jokel, M., Rehman, A., Vass, I., Allahverdiyeva, Y., & Aro, E.-M. (2014). Flavodiiron Protein Flv2/Flv4-Related Photoprotective Mechanism Dissipates Excitation Pressure of PSII in Cooperation with Phycobilisomes in Cyanobacteria. *Plant Physiology*, *164*(2), 805–818. https://doi.org/10.1104/pp.113.231969

Bersanini, L., Allahverdiyeva, Y., Battchikova, N., Heinz, S., Lespinasse, M., Ruohisto, E., … Aro, E. M. (2017). Dissecting the Photoprotective Mechanism Encoded by the *flv4-2* Operon: a Distinct Contribution of Sll0218 in Photosystem II Stabilization. *Plant Cell and Environment*, *40*(3), 378–389. https://doi.org/10.1111/pce.12872

Borges, P. T., Romão, C. V., Saraiva, L. M., Gonçalves, V. L., Carrondo, M. A., Teixeira, M., & Frazão, C. (2019). Analysis of a new flavodiiron core structural

arrangement in Flv1-ΔFlR protein from *Synechocystis* sp. PCC6803. *Journal of structural biology*, *205*(1), 91-102. https://doi.org/10.1016/j.jsb.2018.11.004

Cassier-Chauvat, C., & Chauvat, F. (2014). Function and Regulation of Ferredoxins in the Cyanobacterium, *Synechocystis* PCC6803: Recent Advances. *Life*, *4*(4), 666–680. https://doi.org/10.3390/life4040666

Chaux, F., Burlacot, A., Mekhalfi, M., Auroy, P., Blangy, S., Richaud, P., & Peltier, G. (2017). Flavodiiron Proteins Promote Fast and Transient O_2 Photoreduction in *Chlamydomonas*. *Plant Physiology*, *174*(3), 1825–1836. https://doi.org/10.1104/pp.17.00421

Chukhutsina, V., Bersanini, L., Aro, E. M., & Van Amerongen, H. (2015). Cyanobacterial *flv4-2* operon-encoded proteins optimize light harvesting and charge separation in photosystem II. *Molecular Plant*, *8*(5), 747–761. https://doi.org/10.1016/j.molp.2014.12.016

Cooley, J. W., & Vermaas, W. F. J. (2001). Succinate Dehydrogenase and Other Respiratory Pathways in Thylakoid Membranes of *Synechocystis* sp. strain PCC 6803: Capacity Comparisons and Physiological Function. *Journal of Bacteriology*, *183*(14), 4251–4258. https://doi.org/10.1128/JB.183.14.4251-4258.2001

Di Matteo, A., Scandurra, F. M., Testa, F., Forte, E., Sarti, P., Brunori, M., & Giuffrè, A. (2008). The O_2-scavenging flavodiiron protein in the human parasite *Giardia intestinalis*. *Journal of Biological Chemistry*, *283*(7), 4061–4068. https://doi.org/10.1074/jbc.M705605200

Eisenhut, M., Georg, J., Klähn, S., Sakurai, I., Mustila, H., Zhang, P., … Aro, E. M. (2012). The antisense RNA As1-flv4 in the cyanobacterium *Synechocystis* sp. PCC 6803 prevents premature expression of the *flv4-2* operon upon shift in

inorganic carbon supply. *Journal of Biological Chemistry*, *287*(40), 33153–33162. https://doi.org/10.1074/jbc.M112.391755

Ermakova, M., Battchikova, N., Allahverdiyeva, Y., & Aro, E. M. (2013). Novel heterocyst-specific flavodiiron proteins in *Anabaena* sp. PCC 7120. *FEBS Letters*, *587*(1), 82–87. https://doi.org/10.1016/j.febslet.2012.11.006

Ermakova, M., Huokko, T., Richaud, P., Bersanini, L., Howe, C. J., Lea-Smith, D., … Allahverdiyeva, Y. (2016). Distinguishing the roles of thylakoid respiratory terminal oxidases in the cyanobacterium *Synechocystis* sp. PCC 6803. *Plant Physiology*, *171*, 1307-1319. https://doi.org/10.1104/pp.16.00479

Folgosa, F., Martins, M. C., & Teixeira, M. (2018). Diversity and complexity of flavodiiron NO/O 2 reductases. *FEMS Microbiology Letters Physiology & Biochemistry*, *365*, 1–8. https://doi.org/10.1093/femsle/fnx267

Gerotto, C., Alboresi, A., Meneghesso, A., Jokel, M., Suorsa, M., Aro, E.-M., & Morosinotto, T. (2016). Flavodiiron proteins act as safety valve for electrons in *Physcomitrella patens*. *Proceedings of the National Academy of Sciences*, *113*(43), 12322–12327. https://doi.org/10.1073/pnas.1606685113

Gómez, R., Carrillo, N., Morelli, M. P., Tula, S., Shahinnia, F., Hajirezaei, M. R., & Lodeyro, A. F. (2018). Faster photosynthetic induction in tobacco by expressing cyanobacterial flavodiiron proteins in chloroplasts. *Photosynthesis Research*, *136*(2), 129–138. https://doi.org/10.1007/s11120-017-0449-9

Gonçalves, V. L., Vicente, J. B., Saraiva, L. M., & Teixeira, M. (2011). Flavodiiron proteins and their role in cyanobacteria. In Peschek G., Obinger C., Renger G. (eds) *Processes of Cyanobacteria* (pp. 631-653). Springer, Dordrecht. https://doi.org/10.1007/978-94-007-0388-9_22

Hackenberg, C., Huege, J., Engelhardt, A., Wittink, F., Laue, M., Matthijs, H. C. P., … Hagemann, M. (2012). Low-carbon acclimation in carboxysome-less and photorespiratory mutants of the cyanobacterium *Synechocystis* sp. strain PCC 6803. *Microbiology*, *158*(2), 398–413. https://doi.org/10.1099/mic.0.054544-0

Hanke, G. T., Satomi, Y., Shinmura, K., Takao, T., & Hase, T. (2011). A screen for potential ferredoxin electron transfer partners uncovers new, redox dependent interactions. *Biochimica et Biophysica Acta - Proteins and Proteomics*, *1814*(2), 366–374. https://doi.org/10.1016/j.bbapap.2010.09.011

Helman, Y., Tchernov, D., Reinhold, L., Shibata, M., Ogawa, T., Schwarz, R., … Kaplan, A. (2003). Genes encoding A-type flavoproteins are essential for photoreduction of O2 in cyanobacteria. *Current Biology*, *13*(3), 230–235. https://doi.org/10.1016/S0960-9822(03)00046-0

Holland, S. C., Kappell, A. D., & Burnap, R. L. (2015). Redox changes accompanying inorganic carbon limitation in *Synechocystis* sp. PCC 6803. *Biochimica et Biophysica Acta - Bioenergetics*, *1847*(3), 355–363. https://doi.org/10.1016/j.bbabio.2014.12.001

Howitt, C. A., & Vermaas, W. F. J. (1998). Quinol and cytochrome oxidases in the cyanobacterium *Synechocystis* sp. PCC 6803. *Biochemistry*, *37*(51), 17944–17951. https://doi.org/10.1021/bi981486n

Ilík, P., Pavlovič, A., Kouřil, R., Alboresi, A., Morosinotto, T., Allahverdiyeva, Y., … Shikanai, T. (2017). Alternative electron transport mediated by flavodiiron proteins is operational in organisms from cyanobacteria up to gymnosperms. *New Phytologist*, *214*(3), 967–972. https://doi.org/10.1111/nph.14536

Jokel, M., Johnson, X., Peltier, G., Aro, E. M., & Allahverdiyeva, Y. (2018). Hunting the main player enabling *Chlamydomonas reinhardtii* growth under fluctuating light. *Plant Journal*, *94*(5), 822–835. https://doi.org/10.1111/tpj.13897

Mustila, H., Paananen, P., Battchikova, N., Santana-Sánchez, A., Muth-Pawlak, D., Hagemann, M., … Allahverdiyeva, Y. (2016). The flavodiiron protein Flv3 functions as a homo-oligomer during stress acclimation and is distinct from the Flv1/Flv3 hetero-oligomer specific to the O_2 photoreduction pathway. *Plant and Cell Physiology*, *57*(7), 1468–1483. https://doi.org/10.1093/pcp/pcw047

Ogawa, T. (1991). A gene homologous to the subunit-2 gene of NADH dehydrogenase is essential to inorganic carbon transport of *Synechocystis* PCC6803. *Proceedings of the National Academy of Sciences*, *88*(10), 4275–4279. https://doi.org/10.1073/pnas.88.10.4275

Ohkawa, H., Pakrasi, H. B., & Ogawa, T. (2000). Two types of functionally distinct NAD(P)H dehydrogenases in *Synechocystis* sp. strain PCC6803. *Journal of Biological Chemistry*, *275*(41), 31630–31634. https://doi.org/10.1074/jbc.M003706200

Ort, D. R., & Baker, N. R. (2002). A photoprotective role for O_2 as an alternative electron sink in photosynthesis? *Current Opinion in Plant Biology*, *5*(3), 193–198. https://doi.org/10.1016/S1369-5266(02)00259-5

Peden, E. A., Boehm, M., Mulder, D. W., Davis, R., Old, W. M., King, P. W., … Dubini, A. (2013). Identification of global ferredoxin interaction networks in *Chlamydomonas reinhardtii*. *Journal of Biological Chemistry*, *288*(49), 35192–35209. https://doi.org/10.1074/jbc.M113.483727

Romão, C. V., Vicente, J. B., Borges, P. T., Frazão, C., & Teixeira, M. (2016). The dual function of flavodiiron proteins: Oxygen and/or nitric oxide reductases.

Journal of Biological Inorganic Chemistry, *21*(1), 39–52. https://doi.org/10.1007/s00775-015-1329-4

Schuller, J., Birrel, J., Tanaka, H., Konuma, T., Wulfhorst, H., Cox, N., …Nowaczyk, M. (2019) Structural adaptations of photosynthetic complex I enable ferredoxin-dependent electron transfer. *Science*, *363*(6424), 257-260

Shimakawa, G., Ishizaki, K., Tsukamoto, S., Tanaka, M., Sejima, T., & Miyake, C. (2017). The Liverwort, *Marchantia*, Drives Alternative Electron Flow Using a Flavodiiron Protein to Protect PSI. *Plant Physiology*, *173*, 1636-1647. https://doi.org/10.1104/pp.16.01038

Shimakawa, G., Shaku, K., Nishi, A., Hayashi, R., Yamamoto, H., Sakamoto, K., … Miyake, C. (2015). FLAVODIIRON2 and FLAVODIIRON4 Proteins Mediate an Oxygen-Dependent Alternative Electron Flow in *Synechocystis* sp. PCC 6803 under CO_2 -Limited Conditions. *Plant Physiology*, *167*(2), 472–480. https://doi.org/10.1104/pp.114.249987

Summerfield, T. C., & Sherman, L. A. (2008). Global transcriptional response of the alkali-tolerant cyanobacterium *Synechocystis* sp. strain PCC 6803 to a pH 10 environment. *Applied and Environmental Microbiology*, *74*(17), 5276–5284. https://doi.org/10.1128/AEM.00883-08

Trebst, A., Harth, E., & Draber, W. (1970). On a new inhibitor of photosynthetic electron-transport in isolated chloroplasts. *Zeitschrift für Naturforschung B*, *25*(10), 1157-1159. https://doi.org/10.1515/znb-1970-1018

Tyystjärvi, T., Herranen, M., & Aro, E. M. (2001). Regulation of translation elongation in cyanobacteria: Membrane targeting of the ribosome nascent-chain

complexes controls the synthesis of D1 protein. *Molecular Microbiology*, *40*(2), 476–484. https://doi.org/10.1046/j.1365-2958.2001.02402.x

Yamamoto, H., & Shikanai, T. (2019). PGR5-Dependent Cyclic Electron Flow Protects Photosystem I under Fluctuating Light at Donor and Acceptor Sides. *Plant physiology*, *179*(2), 588-600. https://doi.org/10.1104/pp.18.01343

Yan, J., Kurisu, G., & Cramer, W. A. (2006). Intraprotein transfer of the quinone analogue inhibitor 2, 5-dibromo-3-methyl-6-isopropyl-p-benzoquinone in the cytochrome b_6f complex. *Proceedings of the National Academy of Sciences*, *103*(1), 69-74. https://doi.org/10.1073/pnas.0504909102

Yamamoto, H., Takahashi, S., Badger, M. R., & Shikanai, T. (2016). Artificial remodelling of alternative electron flow by flavodiiron proteins in Arabidopsis. *Nature plants*, *2*(3), 16012. https://doi.org/10.1038/nplants.2016.12

Wada, S., Yamamoto, H., Suzuki, Y., Yamori, W., Shikanai, T., & Makino, A. (2017). Flavodiiron protein substitutes for cyclic electron flow without competing CO_2 assimilation. *Plant Physiology*, *176*, 1509-1518. https://doi.org/10.1104/pp.17.01335

Wang, H. L., Postier, B. L., & Burnap, R. L. (2004). Alterations in Global Patterns of Gene Expression in *Synechocystis* sp. PCC 6803 in Response to Inorganic Carbon Limitation and the Inactivation of ndhR, a LysR Family Regulator. *Journal of Biological Chemistry*, *279*(7), 5739–5751. https://doi.org/10.1080/02670844.2015.1104100

Wasserfallen, A., Ragettli, S., Jouanneau, Y., & Leisinger, T. (1998). A family of flavoproteins in the domains archaea and bacteria. *European Journal of*

Biochemistry, *254*(2), 325–332. https://doi.org/10.1046/j.1432-1327.1998.2540325.x

Williams, J. G. (1988) Construction of specific mutations in photosystem II photosynthetic reaction center by genetic engineering methods in Synechocystis 6803. In Packer L., Glazer A. N. (eds) *Methods in enzymology* (Vol. 167, pp. 766-778). Academic Press. https://doi.org/10.1016/0076-6879(88)67088-1

Vicente, J. B., Gomes, C. M., Wasserfallen, A., & Teixeira, M. (2002). Module fusion in an A-type flavoprotein from the cyanobacterium *Synechocystis* condenses a multiple-component pathway in a single polypeptide chain. *Biochemical and Biophysical Research Communications*, *294*(1), 82–87. https://doi.org/10.1016/S0006-291X(02)00434-5

Zhang, P., Battchikova, N., Jansen, T., Appel, J., Ogawa, T., Aro, E.-M. (2004). Expression and Functional Roles of the Two Distinct NDH-1 Complexes and the Carbon Acquisition Complex NdhD3/NdhF3/CupA/Sll1735 in *Synechocystis* sp. PCC 6803. *The Plant Cell*, *16*(12), 3326–3340. https://doi.org/10.1105/tpc.104.026526

Zhang, P., Eisenhut, M., Brandt, A.-M., Carmel, D., Silen, H. M., Vass, I., … Aro, E.-M. (2012). Operon *flv4-flv2* Provides Cyanobacterial Photosystem II with Flexibility of Electron Transfer. *The Plant Cell*, *24*(5), 1952–1971. https://doi.org/10.1105/tpc.111.094417

Zhang, P., Allahverdiyeva, Y., Eisenhut, M., & Aro, E. M. (2009). Flavodiiron proteins in oxygenic photosynthetic organisms: Photoprotection of photosystem II by FIv2 and FIv4 in Synechocystis sp. PCC 6803. *PLoS ONE*, *4*(4). https://doi.org/10.1371/journal.pone.0005331

Figure supplements and source data files available

Figure 1-Figure supplement 1. *O_2 photoreduction rates under high CO_2.*

Figure 2-Figure supplement 1. *O_2 photoreduction rates during the dark-to-light transition of WT cells with and without addition of 1.5 mM $NaHCO_3$ prior MIMS measurements.*

Figure 2-Figure supplement 2. *O_2 photoreduction rates of the Δ*flv2* and Δ*sll0218* mutants grown at LC pH 7.5* and 8.2 *with and without Na_2CO_3.*

Figure 3-Figure supplement 1. *O_2 uptake in the WT, flv4-2/OE, Δ*flv4* and Δ*cyd* mutant.*

Figure 4-Figure supplement 1. *Growth curves of the different Flv mutants under fluctuating light intensities.*

Figure 1-source data 1. *O_2 reduction rates of WT, flv4-2/OE and M55 mutants grown* in different CO_2 levels.

Figure 2-source data 1. *O_2 reduction rates of WT and FDP mutants grown at different pH levels.*

Figure 3-source data 1. *Transcript abundance of flv1, flv2, flv3 and flv4 genes.*

Figure 4-source data 1. *Growth of the different FDPs mutants under fluctuating light intensities*

Figure 5-source data 1. *Rates of O_2 reduction in response to increasing light intensity in WT, Δ*flv1*/Δ*flv3* and Δ*flv4* mutant cells.*

Figure 6-source data 1. *Rates of O_2 reduction of WT, Δ*flv1*/Δ*flv3* and Δ*flv4* mutant cells grown at different inoculum size.*